NEW DATA ON THE EVOLUTION OF THE NEOTETHYAN OCEANIC BRANCHES IN TURKEY: LATE JURASSIC RIDGE SPREADING IN THE INTRA-PONTIDE BRANCH

M. Cemal Göncüoğlu*,✉, Semih Gürsu, U. Kagan Tekin*** and Serhat Köksal****

   * *Geological Engineering Department, Middle East Technical University, Ankara, Turkey.*
  ** *General Directorate of Mineral Research and Exploration, Natural History Museum, Ankara, Turkey.*
 *** *Geological Engineering Department, Hacettepe University, Ankara, Turkey.*
**** *Central Laboratory, Middle East Technical University, Ankara, Turkey.*
   ✉ *Corresponding author, e-mail: mcgoncu@metu.edu.tr*

ABSTRACT

Tectonically disrupted outcrops of a mélange (Arkotdağ Mélange) between the Rhodope-Pontide and Sakarya micro-continents in NW Anatolia are considered as remnants of the little-known Intra-Pontide oceanic branch of Neotethys. A tectonic sliver of this mélange to the east of the town of Bolu comprises a mega-block of massive and pillow lavas that includes radiolarian chert interlayers and intra-pillow mudstones. The silicified mudstones from the upper part of an intact section yielded moderately preserved but diverse radiolarians of late Kimmeridgian to early Tithonian age.

Geochemical data (major, trace and REE) obtained from the tholeiitic basalts suggest generation in a mid-ocean ridge setting. Magma was likely derived from a spinel lherzolite source by 5-10% partial melting and fractional crystallization processes. The Nd isotopic data suggests heterogeneity of the source. Combined with comparative evidence from a number of similar mélanges along the inferred suture belt in NW Anatolia, it is concluded that the ridge-spreading in the Intra-Pontide Ocean continued at least from middle Middle Jurassic to middle Late Cretaceous.

INTRODUCTION

The Neotethyan oceanic branches in NW Turkey has been the topic of several studies (e.g., Şengör and Yılmaz, 1981; Yılmaz et al., 1995; 1997; Göncüoğlu et al., 1997; Okay and Tüysüz, 1999; Stampfli, 2000; Robertson, 2004; Robertson and Ustaömer, 2004). The initial suggestion of Şengör et al. (1984) is that the northern branch of Neotethys was represented by two oceanic seaways. From north to south these are Intra-Pontide Ocean (IPO) between the Rhodope-Pontide (Fig. 1a) and the Sakarya and the Izmir - Ankara - Erzincan Ocean between Sakarya and the Tauride-Anatolide terranes. The geological history of the Izmir-Ankara Ocean as well as its western (Vardar Ocean in broader sense) and eastern (Erzincan - Sevan - Akera) continuation had been well-documented (for a brief review see Göncüoğlu et al., 2006a; 2006b; 2007). The IPO as proposed by Şengör and Yılmaz (1981), however, is poorly known even though its suture is a "profound stratigraphic, metamorphic and structural boundary (e.g., Okay and Tüysüz, 1999)". Its geological setting, age, evolution and even presence is a matter of debate (e.g., Kaya and Kozur, 1987; Elmas and Yigitbas, 2001; Moix et al., 2008). Published suggestions on the paleogeographic setting, opening and closure ages and the subduction polarity of the IPO are controversial. The tectonic scenarios proposed (Şengör and Yılmaz, 1981; Göncüoğlu et al., 1987; Yılmaz, 1990; Göncüoğlu and Erendil, 1990; Yılmaz et al., 1995; 1997; Elmas and Yigitbas, 2001; Robertson and Ustaömer, 2004) are based on a few local field-studies (e.g., Göncüoğlu and Erendil, 1990, Yılmaz et al., 1997; Elmas et al., 1997; Yigitbas et al., 1999). The basis of these scenarios is a discontinuous sedimentary mélange between the Sakarya and the Rhodope-Pontide continental microplates (Fig. 1b), including blocks of cherts, recrystallized limestones, basic vol-

canic rocks and rarely serpentinites and ultramafic rocks (e.g., Arkotdağ Mélange of Tokay (1973) and Abant Complex of Yılmaz et al. (1982)).

As recently reviewed by Robertson and Ustaömer (2004) and Ustaömer and Robertson (2005), the main tectonic hypotheses for the formation of this mélange are: (1) the oceanic material is of Precambrian age and no sea-floor spreading was realized since then (Kaya, 1977); (2) the mélanges are formed during the closure of the IPO that existed in Mesozoic between the Sakarya microcontinent to the south and the Rhodope-Pontide terrane to the north and closed by northward (Sengör and Yılmaz, 1981; Göncüoğlu et al., 1987; Yılmaz, 1990; Yılmaz et al., 1997; Elmas and Yigitbas, 2001; Robertson and Ustaömer, 2004) or southward (Robertson and Ustaömer, 2004) subduction. A variant of this hypothesis is (3) the oblique northward subduction (Göncüoğlu and Erendil, 1990); the IPO was formed as an embayment within the Izmir - Ankara Ocean (Okay et al., 1996; 2006); (4) no evidence exists for the IPO to the north of the Sakarya Terrane (Moix et al., 2008). In this scenario, the mélanges formed during the closure of the Neotethyan Izmir - Ankara Ocean to the south of Sakarya Terrane and were emplaced to their present position by strike-slip faulting (Elmas and Yigitbas, 2001).

These contrasting ideas are due to the fact that the Intra-Pontide Suture (IPS) complex is not yet studied in detail in regard to the constituting rock-units. In addition to the pre-neotectonic geological complexity, the suture belt is juxtaposed with the branches North Anatolian Transform Fault (Fig. 1b) and the original features of this suture complex are largely erased (e.g., Göncüoğlu et al., 1997). Moreover, the data on the geochemical characteristics and ages of the basic volcanic rocks in the mélange are scattered and difficult to interpret.
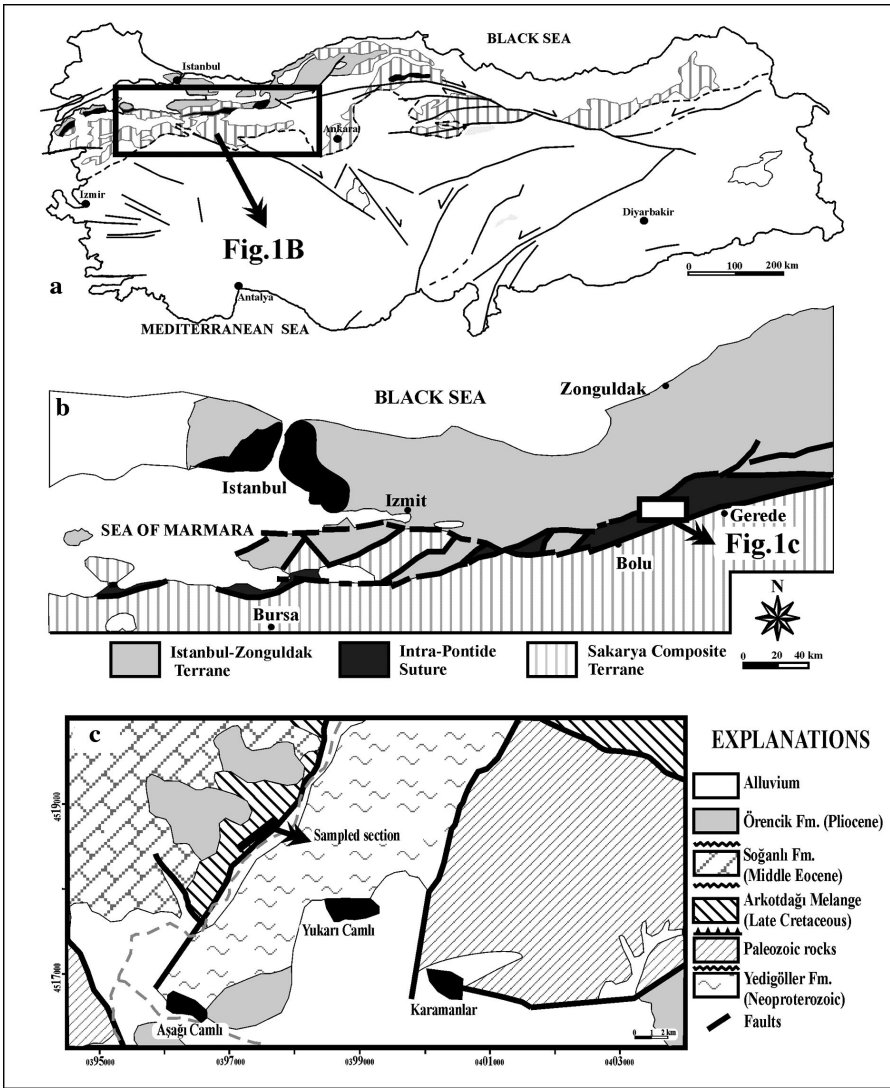
Fig. 1 - a) Location of the Intra-Pontide Suture Belt and surrounding terranes in North Anatolia (modified after Göncüoğlu et al., 1997); b) Tectonic map of NW Anatolia and the location of the study area (modified after Elmas and Yigitbas, 2001). c- Geological map of the study area (modified after Sevin et al., 2002).

In this study, we report the first detailed geochemical data from the basalts and micro-palaeontological evidence from associated radiolarian limestones within the IPS mélange complex in Bolu area. Based on these new data, we then discuss the proposed models on the geological evolution of the IPS and correlate it with the surrounding NW Anatolian subduction-accretion complexes. This study is important because it provides solid evidence for the evolution of the IPO.

GEOLOGICAL FRAMEWORK

Rock-units studied are located to the east of the town of Bolu (Figs. 1b, c), along the Bolu - Mengen road within the Kocaçay Valley, along one of the main strands of the North Anatolian Transform Fault. The original contacts of the rock-units in this area are affected by oblique and strike-slip movements within the still active North Anatolian Transform Fault. The studied rocks occur as tectonic slivers of variable size and represent dismembered parts of an Upper Cretaceous mélange, which is known as Arkotdağ Mélange (Tokay, 1973) to the east and Abant Complex (Yılmaz et al., 1982) to the west of Bolu. The mélange character of the formation was first recognized by Blumenthal (1949). To the south of the North Anatolian Transform Fault, the

Arkotdağ Mélange is thrust upon the Lower Cretaceous pelagic limestones (Sogukcam Formation) that belong to the northern slope of the Sakarya microcontinent. In the study area (Fig. 1c), the representatives of the Arkotdağ Mélange are imbricated with basement rocks of the Istanbul - Zonguldak Terrane of the Rhodope-Pontide unit and their Eocene cover. The basement rocks of the Istanbul - Zonguldak Terrane in the studied area include Late Neoproterozoic meta-ophiolites and arc-related rocks, known as the Bolu Massif (e.g., Ustaömer and Rogers, 1999). A tectonically disrupted series of Ordovician - Silurian siliciclastics and Devonian - Carboniferous recrystallized limestones constitute the Paleozoic cover. The Jurassic - Lower Cretaceous sediments of the Istanbul - Zonguldak Terrane, are mainly represented by sandstones and volcanoclastic rocks to the North of Bolu, known as the Yemisliçay Formation (e.g., Sevin et al., 2002), were not encountered in the study area.

The Arkotdağ Mélange is composed of a sedimentary mélange with blocks of serpentinites, gabbros, and pillow-basalts, pelagic limestones and radiolarian cherts. To the SE of the study area, the unit is several (3-8) kilometers thick and associated with intensively deformed and slightly metamorphosed debris flows. Its contact with the rock-units of the Bolu Massif of the Istanbul - Zonguldak Terrane is always fault-related. The oldest Paleogene rocks in the Kocaçay Valley are known as the Soganlı Formation, compris-

ing sandstones and limestones of Middle Eocene. The Soganlı Formation unconformably overlies both the Arkotdağ Mélange and the Bolu Massif and hence postdates the initial juxtaposition of the Arkotdağ Mélange of the IPO and the continental crust of the Istanbul - Zonguldak Terrane.

Samples analyzed in this study are volcanic and sedimentary rocks that occur within the mélange on the Bolu-Gokcesu. The outcrop is about 7 km long and 1.5 km wide. It forms a tectonically disrupted complex with blocks of gray siltstones and greenish shales, basalts, red radiolarian cherts, sheared serpentinites and pink to red micritic limestones alternating with greenish altered pillow-basalts (Figs. 2a, b). Infrequently, the mélange includes radiolarian chert blocks in a matrix of debris flow deposits. The size of these blocks ranges between 0.5-8m.

A single block with more or less continuous succession of volcanic rocks alternating with sediments was measured and sampled (Fig. 1c). Individual chert layers in the studied block reach up to 1.5 meters. The cherts are intensively folded, thinly-bedded and include brick-red and violet mudstone alternations. The pillow-lavas are alternating with massive lavas and cut by diabase dykes. The rims of the pillows include calcite-filled amygdales. Intra-pillow-fillings of red chert and greenish hyaloclastics are common. The starting and end-points of the section is: 0397546 N/ 451863 E and 0397654 N/ 4518797E, respectively. The columnar section of the measured section with the sample locations of petrologic and paleontological samples is given in Fig. 3. The section is bounded by shear-zones towards the melange units and comprises massive lavas interlayered with thin chert bands in its lower part (Fig. 3). A thick interval of pillow lavas with rare micritic limestone lenses and radiolarian chert bands constitutes the middle part of the sequence. The upper part, from where the fossil-bearing sample is taken, is dominated by red radiolarian cherts with thin mudstone interlayers. The upper contact of the section is another shear-zone with foliated and serpentinized mafic rocks.

PETROGRAPHY

The basaltic samples that were analyzed are commonly amygdaloidal and contain rarely subhedral plagioclase phenocrysts (< 5%, generally 0.32-0.96 mm) which are set in a fine-grained groundmass (Fig. 4a). The plagioclase laths in the groundmass generally are occupied by chloritized wedge shaped glass and between others by fine grained anhedral clinopyroxene (0.02-0.06 mm) and ± olivine (0.02-0.03 mm) crystals as interstitial texture (both intersertal and intergranular) co-exits in the samples (Fig. 4b). Primary magnetite rarely occurs as subhedral grains. Plagioclase phenocrysts and laths are albite in composition and the amygdales are mainly filled with secondary calcite minerals. The calcite + quartz + chlorite + epidote mineral assemblage are observed in the fractured zones and the groundmass which is altered to clay minerals (partly chlorite) related to the hydrothermal alterations.

GEOCHEMISTRY OF BASALTIC ROCKS

Methods

From several whole-rock samples analyzed in Geochemistry Laboratories of Acme in Canada (Vancouver) using their standard analytical procedures, eleven fresh and repre-

sentative samples were considered. Major, trace and rare earth elements (REE) were determined by using inductively coupled plasma atomic emission spectrometry (ICP-AES) after fusion with $LiBO_2/Li_2B_4O_7$ and inductively coupled plasma-mass spectrometry (ICP-MS) after acid decomposition (HNO_3 of 5%), respectively. The results are shown in Table 1. Major elements detection limits are (in wt.%): SiO_2, Al_2O_3, MgO, CaO, Na_2O, K_2O, MnO, TiO_2 = 0.01; Fe_2O_3 = 0.04; P_2O_5, Cr_2O_3 = 0.001-0.002; LOI = 0.10. Trace elements and REE detection limits are (in ppm): V = 8; Ba, Sn = 1; Sr, Gd, W = 0.5; Nd = 0.3; Co = 0.2; Cs, Hf, Nb, Rb, Ta, U, Y, Zr, Th, La, Ce = 0.1; Sm, Dy, Yb = 0.05; Er = 0.03; Pr, Eu, Ho = 0.02; Tb, Tm, Lu = 0.01. Analytical pre-
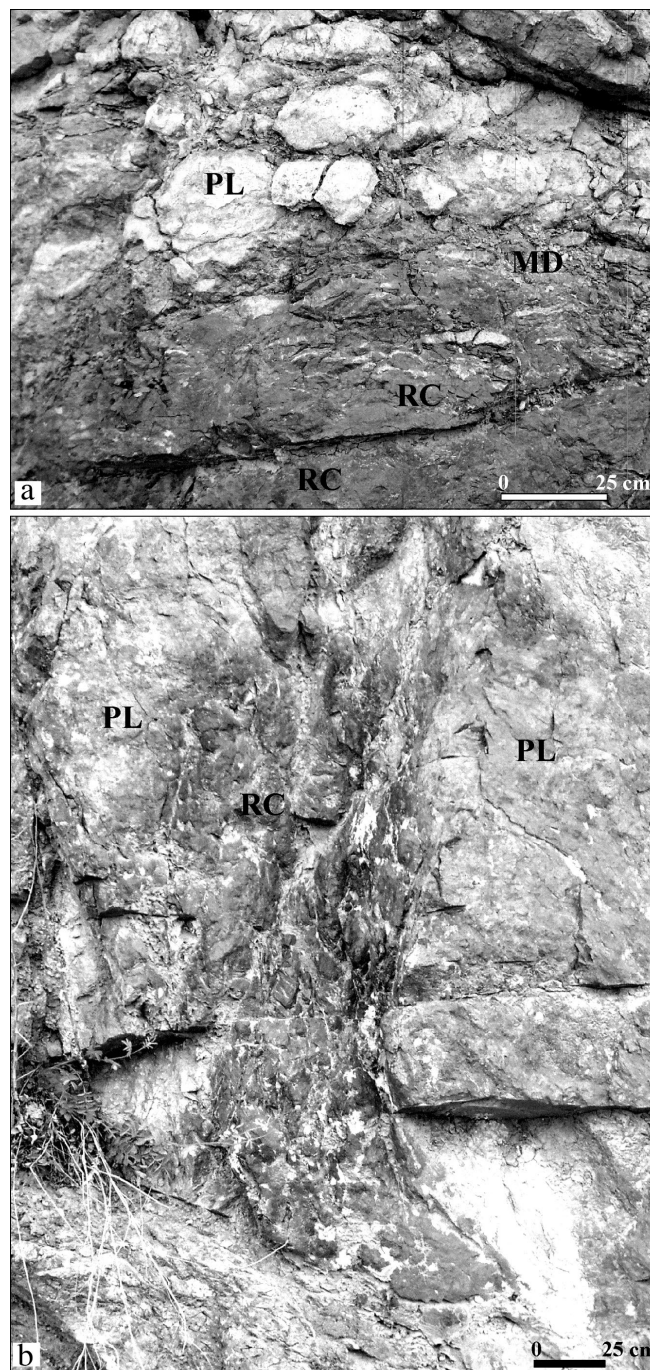

Fig. 2 - Field-view of the basaltic rocks and associated radiolarian cherts. a) Alternation of pillow-lavas and thin-bedded mudstones and radiolarian cherts. b) Deformed radiolarian chert lens between pillow-lavas. PL-pillow-lavas, RC-radiolarian chert, MD-mudstone.

cision is 0.05 - 0.15% for major elements and 0.5 - 1.5% for trace elements and REE.

Isotope geochemistry analyses (Sr-Nd) were performed at the Radiogenic Isotope Laboratory of Middle East Technical University Central Laboratory (Ankara, Turkey). The analytical procedures were described in detail by Köksal and Göncüoğlu (2008). Isotope ratios were measured by a Triton TI Mass Spectrometer using static multi-collection. $^{87}Sr/^{86}Sr$ and $^{143}Nd/^{144}Nd$ data are normalized with $^{86}Sr/^{88}Sr$ = 0.1194, and $^{146}Nd/^{144}Nd$ = 0.7219, respectively. Analytical uncertainties are given at $2\sigma_m$ level. During the course of the measurement Sr NIST SRM 987 and Nd La Jolla was measured as 0.710243 ± 6 and 0.511850 ± 2, respectively. No corrections for instrumental bias were applied to Nd and Sr isotopic compositions.

Whole rock geochemistry

All studied samples are variably affected by alteration, as reflected by the petrographic observations and the scatter of alkali elements (e.g., Na_2O: 3.02-5.31 wt.% and K_2O: 0.04-0.21 wt.%). Hence, the rocks have experienced element mobility, particularly of large ion lithophile elements (LILE) (e.g., Floyd et al., 2000). However, some high field strength elements (HFSE) and rare earth elements (REE) can be utilized to determine the petrogenetic features and source characteristics of the magmatic rocks, as they are relatively immobile (e.g., Pearce and Cann, 1973; Floyd and Winchester, 1978; Floyd et al., 2000). By this, only these immobile HFSE (i.e., Ce, Y, Nb, Zr, Ti, Ta and Yb) and REE were used for the petrogenetic discriminations and interpretations.

The studied samples plot in the sub-alkaline basalts field based on Zr/TiO_2 - Nb/Y diagram (Winchester and Floyd, 1977) (Fig. 5). The incompatible elements as Nb (1.8-4.8 ppm) and Y (27.5-46.4 ppm) show a general decrease with Zr (82.2-142.9 ppm) as an index of differentiation (Table 1), which is related to the clinopyroxene + plagioclase fractionation.

In terms of high field strength elements, the tholeiitic basalts are more akin to normal mid-ocean ridge basalts (N-MORB; Sun and McDonough, 1989) than enriched mid-ocean ridge basalts (E-MORB) and oceanic island basalts (OIB). The chondrite normalized multi-element pattern of tholeiitic basalts are slightly enriched in Th, Nb elements and display positive anomalies in light REE (LREE) and heavy REE (HREE) (Fig. 6).

Chondrite normalized multi-element profiles of the studied samples show no geochemical signatures of lithospheric contamination or subduction. The samples are relatively enriched in LREE relative to chondrite (La = 10.5-37.5 x chondrite) (Fig. 6), primitive mantle (La = 3.6-12.9 x primitive mantle) and N-MORB (La = 1-3.5 x N-MORB). Compared with LREE, all samples have significant flattening of REE patterns from Sm to Ho and display Eu anomalies. The marked negative Eu anomaly (($Eu/Eu^*)_N$ = 0.76-0.98) in basalts (Fig. 6) is indicative for extensive fractional crystallization involving plagioclase. Chondrite normalized HREE of the samples show roughly flat unfractionated patterns (Lu = 14.1-27.1 x chondrite; Lu = 4.8-9.3 x primitive mantle; L u= 0.79-1.51 x N-MORB). Chondrite-normalized $(La/Sm)_N$, $(La/Yb)_N$ and $(Gd/Yb)_N$ ratios in basalts are not scattered (0.58-1.43, average 0.84; 0.78-2.10, average 1.12; 1.09-1.48, average 1.26) and have similarities to an N-MORB source (0.55, 0.60, 0.98) rather than E-MORB (1.80, 1.53, 1.02) or OIB (11.58, 2.33, 2.86) (all correlative data from Sun and McDonough, 1989).

An important feature of the chondrite normalized REE pattern is that it reflects a slight enrichment in LREE and displays a flat pattern in MREE and HREE and resembles the N-MORB pattern of Sun and McDonough (1989). The unfractionated HREE and Y patterns clearly show that the parent mafic magmas were produced within the garnet-free field.

To summarize, geochemical signatures of the studied basalts clearly indicate a tholeiitic affinity. All samples have marked depletion in Eu with enrichment of HFSE (high field strength elements). The slightly enriched but parallel pattern in LREE and flattening from MREE to HREE (except Eu) clearly indicate that basalts may have been produced from an N-MORB type source followed by low-grade fractional crystallization.
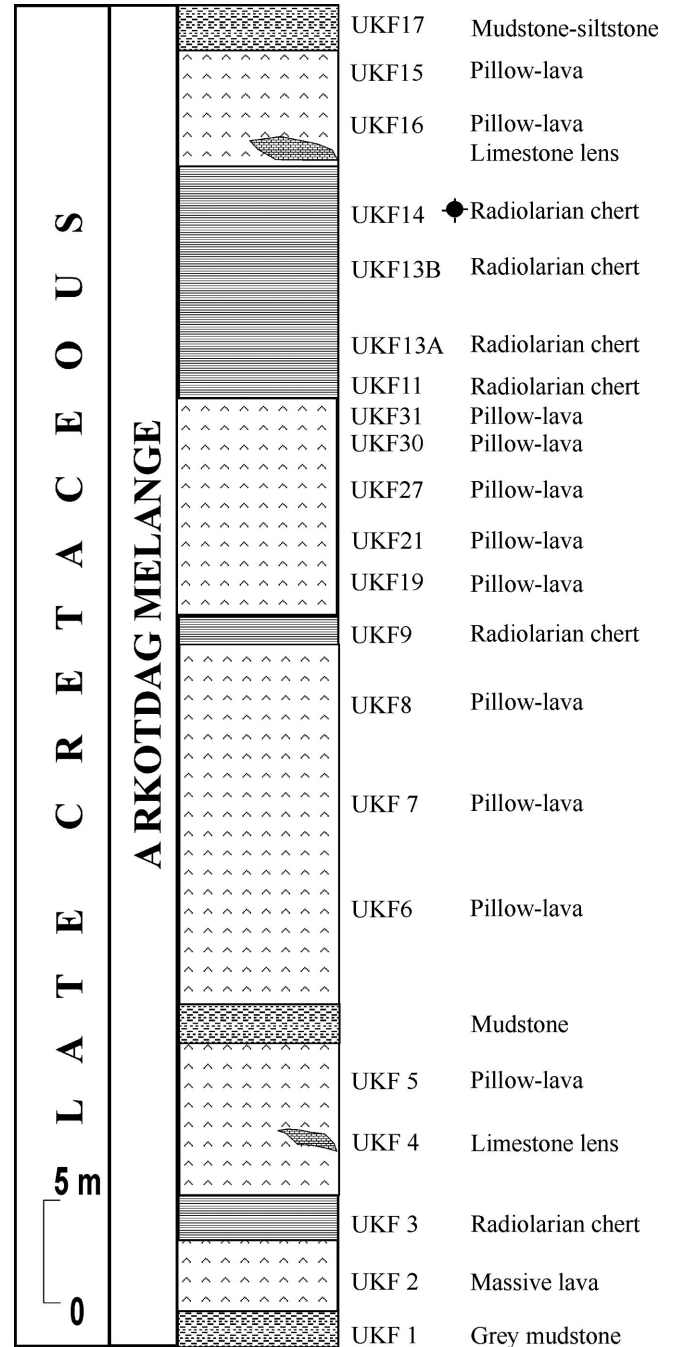

Fig. 3 - Measured columnar section of the sampled succession within the basalt-chert block on the Bolu-Mengen road and location of the studied samples (crossed dot indicates the fossil-bearing sample).

Table 1 - Representative chemical analyses of basalts in the investigated area.

Sample No	UKF5	UKF6	UKF7	UKF8	UKF15	UKF16	UKF19	UKF21	UKF27	UKF30	UKF31
					Major	**Elements,**	**% wt**				
SiO_2	46.10	44.97	45.34	44.76	46.82	46.07	42.92	45.11	46.13	46.01	45.87
$TiO2$	1.84	2.06	2.32	1.57	2.03	1.63	1.50	1.66	1.85	1.30	1.70
Al_2O_3	13.73	14.25	14.14	13.39	13.26	13.76	16.78	14.51	14.00	14.95	14.17
Fe_2O_3	11.58	11.20	10.80	11.23	11.02	9.80	10.22	11.04	12.92	11.29	10.24
MnO	0.23	0.20	0.38	0.30	0.22	0.18	0.19	0.28	0.29	0.31	0.23
MgO	7.05	6.73	6.39	7.20	6.94	5.69	6.06	6.75	7.80	6.82	5.56
CaO	8.50	9.05	9.32	8.05	8.75	11.13	11.53	8.92	6.98	7.27	9.95
Na_2O	4.39	4.25	3.92	5.20	5.31	4.54	3.51	4.35	3.02	4.58	4.12
K_2O	0.04	0.07	0.13	0.10	0.13	0.13	0.19	0.19	0.21	0.08	0.11
P_2O_5	0.15	0.18	0.20	0.13	0.17	0.17	0.18	0.13	0.15	0.12	0.18
Cr_2O_3	0.035	0.030	0.024	0.045	0.035	0.044	0.056	0.042	0.056	0.054	0.043
LOI	6.20	7.0	7.0	7.90	5.50	6.6	6.6	6.6	6.3	6.9	7.6
Total	99.84	99.99	99.96	99.87	100.18	99.74	99.75	99.58	99.68	99.77	99.77
					Trace	**Elements,**	**ppm**				
Pb	2.9	3.3	5.7	30.8	5.1	1.6	1.6	2.1	1.7	2.1	1.3
Ni	79	71.5	66.1	80.8	80.7	117.1	141.4	78.2	86.5	179.3	100
Sc	37	42	39	38	45	39	44	39	50	35	39
Ba	24.1	36.8	64.6	43.5	70.3	24	49	66	39	40	38
Co	43.5	41.4	42.3	41.6	42.8	51.1	57.3	43	48.2	54	44.7
Cs	0.1	0.2	0.2	0.2	0.4	0.2	0.4	0.2	0.3	0.3	0.2
Ga	16.5	17.3	16.5	15.6	16.8	14.9	22.1	15.1	18	17.2	15.5
Hf	3.2	3.5	4.3	2.8	3.8	3.3	2.7	2.9	3.7	2.8	3.1
Nb	2.4	3.3	3.7	2.5	4.8	3.0	2.6	2.6	3.3	1.8	3.0
Rb	0.5	1.2	2.3	1.4	3.2	1.4	3.4	3.8	3.8	1.6	1.6
Sr	194.2	144.4	178.8	200.5	149.1	169.8	111.3	258.4	143.9	295.6	160.5
Ta	0.1	0.2	0.2	0.1	0.3	0.3	0.2	0.2	0.3	0.2	0.3
Th	0.1	0.13	0.14	0.11	0.1	0.2	0.2	0.3	0.2	0.2	0.3
U	0.3	1.0	0.5	0.2	0.3	0.5	0.4	0.1	0.1	0.1	0.2
V	323	353	389	341	331	331	247	315	375	269	251
W	0.7	0.7	0.9	1.1	1.2	0.7	1.0	0.8	0.6	1.1	0.9
Zr	114.8	125.7	142.9	94.6	135.1	118.8	102.2	107.3	115.3	82.2	109.2
Y	40	43	46.4	32.8	44.3	39	26.2	33.1	37.4	27.5	33.6
Ti	11028.9	12347.6	13906.1	9410.6	13366.6						
					Rare Earth	**Elements,**	**ppm**				
La	4.1	8.9	5.0	3.3	6.4	4.3	7.4	3.9	5.9	2.5	4.6
Ce	13.4	21.2	15.7	11.5	16	13.5	13.1	11.7	15.1	7.0	12.2
Pr	2.34	3.17	2.75	2.03	2.78	2.42	2.15	2.09	2.56	1.31	2.21
Nd	12.4	16.5	15.2	10.9	13.2	13.2	11.6	10.6	13.6	7.3	12.6
Sm	4.21	4.70	5.19	3.63	4.18	4.32	3.32	3.50	4.17	2.78	3.73
Eu	1.34	1.54	1.52	1.02	1.31	1.38	1.20	1.07	1.58	0.90	1.29
Gd	5.50	6.12	6.60	4.63	5.22	5.61	4.17	4.67	5.81	3.76	4.98
Tb	1.12	1.23	1.32	0.95	1.02	1.04	0.76	0.94	1.08	0.78	0.94
Dy	6.30	7.02	7.84	5.56	5.86	6.45	4.43	5.55	6.45	4.81	5.95
Ho	1.39	1.46	1.63	1.19	1.19	1.36	0.93	1.24	1.47	1.09	1.20
Er	4.02	4.27	4.73	3.41	3.46	4.01	2.57	3.58	4.21	3.14	3.50
Tm	0.65	0.68	0.77	0.59	0.52	0.64	0.42	0.57	0.64	0.46	0.55
Yb	3.61	3.69	4.24	3.00	2.91	3.93	2.52	3.40	3.76	2.85	3.37
Lu	0.56	0.63	0.69	0.52	0.47	0.58	0.36	0.52	0.59	0.45	0.49
$\sum REE$	60.94	81.11	73.18	52.23	64.52	62.74	54.93	53.33	66.92	39.13	57.61
Nb/Y	0.06	0.076	0.079	0.076	0.108	0.076	0.099	0.078	0.088	0.065	0.089
Th/Yb	0.027	0.035	0.033	0.036	0.034	0.050	0.079	0.088	0.053	0.070	0.089
La/Ce	0.306	0.419	0.318	0.286	0.411	0.318	0.564	0.333	0.390	0.357	0.337
Ce/Y	0.335	0.493	0.338	0.350	0.361	0.346	0.500	0.353	0.403	0.254	0.363
La/Nb	1.708	2.696	1.351	1.320	3.333	1.433	2.846	1.500	1.787	1.388	1.533
Zr/Nb	47.83	38.09	38.62	37.84	28.14	39.6	39.3	41.26	34.94	45.66	36.4
Ti/Yb	3055.1	3346.2	3279.7	3136.8	4593.3	2486	3458	2926.4	2949.1	2734.1	3023.67
Ta/Yb	0.027	0.054	0.047	0.033	0.103	0.076	0.079	0.058	0.079	0.070	0.089
$(La/Yb)_N$	0.81	1.73	0.84	0.79	1.57	0.7848	2.10	0.82	1.12	0.88	0.98
$(La/Sm)_N$	0.62	1.22	0.62	0.58	0.98	0.6425	1.44	0.72	0.91	0.81	0.79
$(Gd/Yb)_N$	1.26	1.37	1.28	1.27	1.48	1.1808	1.37	1.73	1.27	1.09	1.22
(Eu/Eu^*)	0.95	0.88	0.79	0.76	0.85	0.86	0.98	0.81	0.98	0.85	0.93

Chondrite normalization data taken from Sun and McDonough (1989).

To determine the source heterogeneity and/or mixing effects, we used HFSE ratios (e.g., Ce/Y, Nb/Y, Zr/Nb, Ti/Yb, Ta/Yb (e.g., Taylor and McLennan, 1985; Leeman and Hawkesworth, 1986; Hart et al., 1989; Coish and Sinton, 1992). The analyzed samples have similar Ce/Y (0.25-0.5; average 0.37), Nb/Y (0.076-0.108; average 0.081) and higher Zr/Nb (28.14-47.83; average 38.88), Ti/Yb (2486-4593; average 2905.9), Th/Yb (0.027-0.089; average 0.054) and Ta/Yb (0.027-0.10; average 0.65) ratios which correlate well with N-MORB source (Sun and McDonough, 1989) and suggest that crustal contamination has not been significant in the genesis of the mafic magmas. The negative trend in Nb/Y - Zr/Nb
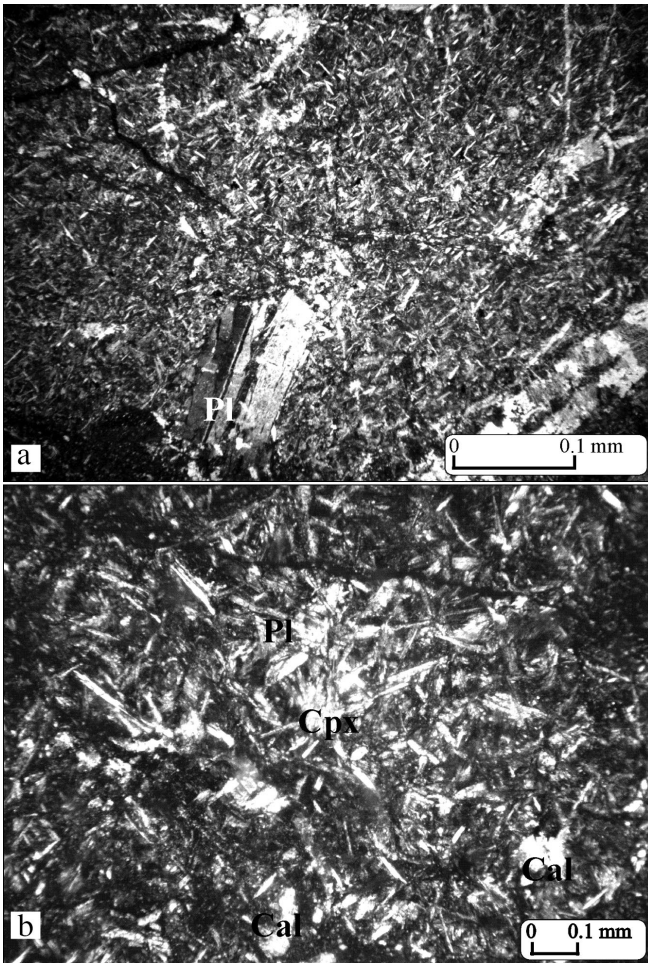
Fig. 4 - a) Microphotographs of the basalts with plagioclase phenocrysts, enclosed within fine-grained groundmass, XPL; b) plagioclase laths are occupied with clinopyroxene minerals with intergranular texture, XPL. (XPL-cross-polarized light, Pl-plagioclase, Cpx-clinopyroxene, Cal-calcite)

Fig. 5 - Zr/TiO$_2$-Nb/Y classification diagram of Winchester and Floyd (1977). (Open squares: basalts).

Fig. 6 - Chondrite normalized multi-element and REE diagrams of the studied samples (open squares). Solid circle: ocean-island basalt (OIB), gray circle: enriched mid-ocean ridge basalt (E-MORB), diamond: normal mid-ocean ridge basalt (N-MORB). Normalization values are from Sun and McDonough (1989).

Fig. 7 - Nb/Y vs. Zr/Nb diagram for basalts, compared with N-MORB, E-MORB and OIB. Symbols as in Fig. 5.

variation also suggests that the observed fractionation is a function of the partial melting of the N-MORB source (Fig. 7). The diagram also shows that the mafic magmas were generated from the partial melting of a N-MORB source and do not imply any source heterogeneity and/or mixing effects.

Various tectonic discrimination diagrams were proposed to determine the geotectonic setting of the basic rocks (e.g., Floyd and Winchester, 1975; Pearce and Norry, 1979). On Zr/Y-Zr binary diagrams (Pearce and Norry, 1979), all studied samples distinctly plot within the MORB field (Fig. 8). Cr-Y variations (Fig. 9a) and negative Eu anomaly in the basalts clearly indicate the fractionation of the Fe-Ti oxides, clinopyroxene and/or olivine and plagioclase fractionation, respectively. Similarly, Cr (164-383 ppm) contents of samples decrease with increasing Y (26.2-46.4 ppm) related to the clinopyroxene and plagioclase differentiation and all samples might be produced by low-degree (< 20%) mantle melting (Fig. 9a).

To determine the partial melting of the source rock, we used MREE/HREE ratios, which can distinguish the spinel and garnet stability fields (e.g., Thirlwall et al., 1994; Baker et al., 1997). Fig. 9b presents (Sm/Yb)$_N$ - (Yb)$_N$ data for the studied basalts for non-modal batch melts of spinel and garnet lherzolite source (spinel lherzolite: 0.578 ol, 0.27 opx, 0.119 cpx, 0.033 sp; garnet lherzolite: 0.598 ol, 0.211 opx, 0.076 cpx, 0.115 gr) (Thirlwall et al., 1994; Baker et al.,
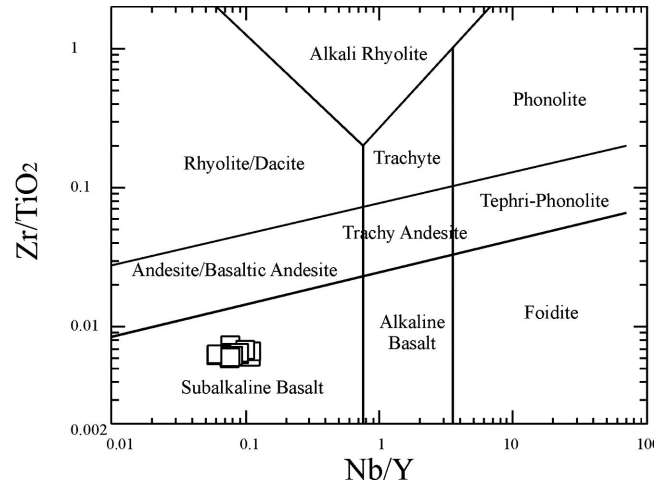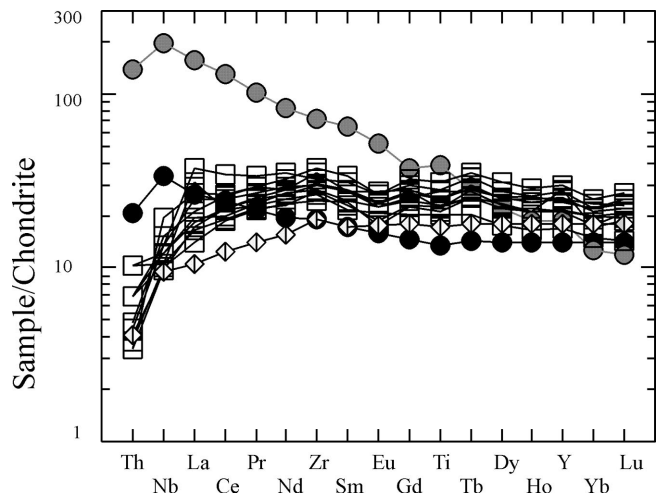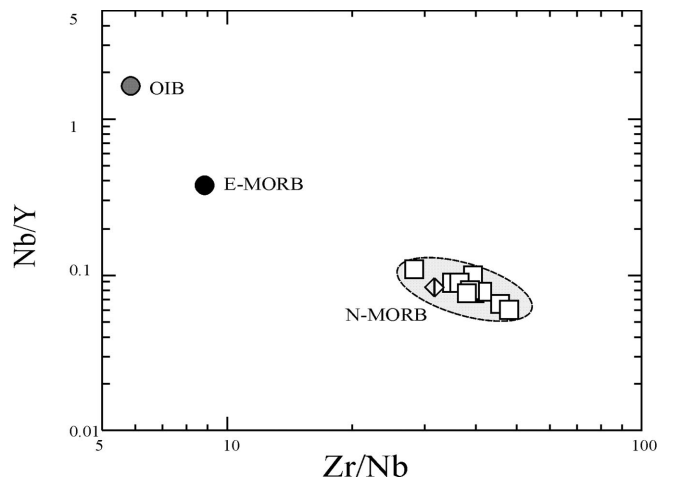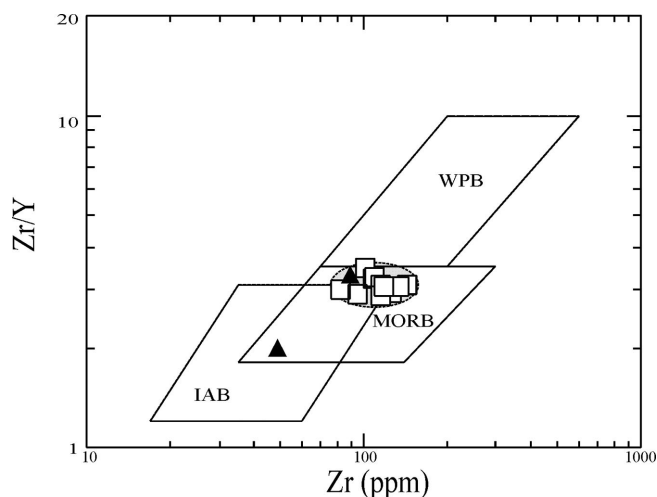
Fig. 8 - Zr/Y vs. Zr discrimination diagram (Pearce and Norry, 1979) of the studied samples. Solid triangle: basaltic rocks of Alacam Melange (data from Robertson and Ustaömer, 2004). N-MORB-normal mid-ocean ridge basalts, WPB-within-plate basalts, IAB-island-arc basalts. Symbols as in Fig. 5.

1997). The primitive mantle source concentrations are taken from Sun and McDonough (1989). The low MREE/HREE [e.g., $(Sm/Yb)_N$] ratio with variable degrees of partial melting are formed by the spinel lherzolite source (about 5-10%) than garnet lherzolite (Fig. 9b). Partial melting of about 5-10% of spinel lherzolite source can be produced significant co-variations in $(Sm/Yb)_N$-$(Yb)_N$ diagram although some scatter in $(Sm/Yb)_N$ array in the studied samples may be accounted to the fractional crystallization process.

To summarize, geochemical and petrogenetic evaluation suggests that the studied basalts were erupted in a MORB-related environment and were produced from a spinel lherzolite source by 5-10% partial melting and fractional crystallization processes.

Sr and Nd isotope geochemistry

Sr and Nd isotopic data determined from the studied basaltic samples are given in Table 2. $(^{87}Sr/^{86}Sr)_i$ ratios of the samples yiel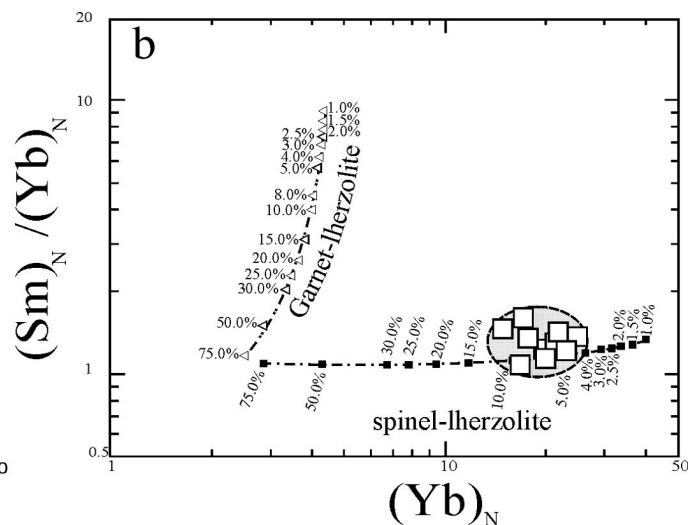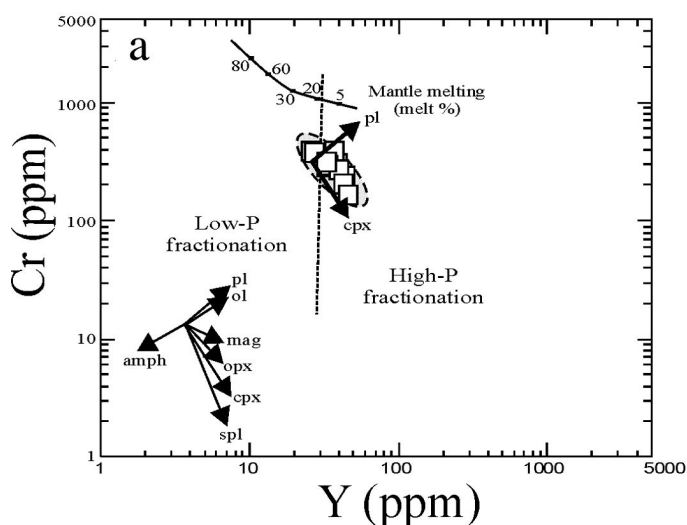d a range of 0.707442-0.709016, which is considerably higher than that of N-MORB (e.g., 0.702540-0.702920; Dupré and Allègre, 1980). The whole-rock geochemical data infer that Rb and Sr are highly mobile, as they do not correlate with the immobile elements. Therefore, the main cause of the elevated $(^{87}Sr/^{86}Sr)_i$ ratios may be the mobility of these elements, although the effects of low temperature seafloor alteration and metamorphism and subsequent radiogenic ingrowth should be considered (e.g., Hoernle, 1998).

High $(^{143}Nd/^{144}Nd)_i$ ratios of the samples, ranging from 0.512471 to 0.512786, are consistent with the whole-rock geochemical data, although slightly lower than the characteristic Nd isotopic data of the N-MORB (e.g., 0.512992-0.513269, Chauvel and Blichert-Toft, 2001). Nd isotopic ratios are not susceptible to seawater alteration or metamorphism (e.g., Hoernle, 1998; Kamenetsky et al., 2000). Therefore, the lower $(^{143}Nd/^{144}Nd)_i$ ratios of the analyzed samples relate to the source characteristics, and are likely due to the heterogeneity in the source melt. The heterogeneity of the mantle, an accepted phenomenon (e.g., Zindler and Hart, 1986; Hofmann, 1989), is valid also for the MORB environments. Potential sources of the mantle heterogeneity are the recycling of oceanic crustal component into the mantle (e.g., Rehkämper and Hofmann, 1997; Hofmann, 2003; Rudge et al., 2005; Sobolev et al., 2007) or partial melting of complex mantle including deep-mantle plume-derived enriched mantle and enriched upper-mantle asthenosphere (e.g., Kamanetsky et al., 2000). For the studied samples, the possible sources/processes decreasing the $(^{143}Nd/^{144}Nd)_i$ ratios is likely to be an earlier subduction of the late Paleozoic - early Mesozoic Tethys (e.g., Paleotethys sensu Şengör and Yılmaz, 1981).

RADIOLARIAN DATA AND DATING

From eleven paleontological samples taken from the studied succession (Fig. 3) and 4 samples from other radiolarian chert blocks within the mélange, moderately preserved but diverse radiolarians were obtained only from a single silicified mudstone in sample UKF-14 in the upper part of the measured section (Fig. 3). Although radiolarian fauna of this

Fig. 9 - a) Cr vs. Y diagram (Floyd et al., 1991) of the studied samples; b) Variation of $(Sm/Yb)_N$-$(Yb)_N$ for the studied samples. Melt curves are non-modal, batch partial melting of garnet and spinel lherzolite source (garnet lherzolite: 0.598 ol, 0.211 opx, 0.076 cpx, 0.115 gr; spinel lherzolite: 57.8 % ol, 27 % opx, 11.9 % cpx, 3.3 % sp (Thirlwall et al., 1994; Baker et al., 1997). Symbols as in Fig. 5. pl: plagioclase, ol: olivine, opx: orthopyroxene, cpx: clinopyroxene, spl: spinel, amph: amphibole.

Table 2 - Sr and Nd isotopic compositions of the studied samples.

Samples	$^{87}Sr/^{86}Sr$	Rb (ppm)	Sr (ppm)	$^{87}Sr/^{86}Sr_{(150)}$	$^{143}Nd/^{144}Nd$	Nd (ppm)	Sm (ppm)	$^{143}Nd/^{144}Nd_{(150)}$	$\varepsilon Nd_{(150)}$
UKF5	0.709032 ± 11	0.5	192.2	0.709016	0.512988 ± 2	12.4	4.21	0.512786	6.66
UKF6	0.707493 ± 9	1.2	144.4	0.707442	0.512665 ± 5	16.5	4.70	0.512496	0.99
UKF7	0.707559 ± 12	2.3	178.8	0.707480	0.512674 ± 5	15.2	5.19	0.512471	0.51
UKF8	0.707686 ± 9	1.4	200.5	0.707643	0.512874 ± 2	10.9	3.63	0.512676	4.51
UKF15	0.707617 ± 8	3.2	149.1	0.707485	0.512945 ± 2	13.2	4.18	0.512757	6.09

sample is mainly dominated by Nassellaria (*Archaeodictyomitra apiarium* (Rüst), *A. excellens* (Tan Sin Hok), *A. minoensis* (Mizutani), *Archaeodictyomitra* sp., *Hsuum* spp., *Cinguloturris cylindra* Kemkin and Rudenko, *C. primorika* Kemkin and Taketani, *Wrangellium okamurai* (Mizutani), *Xitus* sp., *Parvicingula* sp., *Triversus* sp., *Loopus doliolum* Dumitrica *in* Dumitrica et al. (1997), *Loopus* sp., *Syringocapsa* sp., *Sethocapsa accincta* Steiger, *Zhamoidellum ovum* Dumitrica, *Z. ventricosum* Dumitrica and *Pseudoeucyrtis* ? sp.), rare specimens of Spumellaria (*Pantanellium* sp.) was also encountered in the fauna (Plate 1).

Within the fauna, two taxa (*Cinguloturris primorika* and *Archaeodictyomitra excellens*) have first appearance datum in the basal part of late Kimmeridgian (Baumgartner et al., 1995; Kemkin and Taketani, 2004; Fig. 10). This level corresponds to the basal part of UAZ 11 of Baumgartner et al. (1995). Although *Cinguloturris primorika* was not controlled in many localities, *Archaeodictyomitra excellens* is well-known from many Tethyan and Pacific regions (Goriçan, 1994; Baumgartner et al., 1995; Hori, 1999).

Three taxa as *Zhamoidellum ovum*, *Z. ventricosum* and *Wrangellium okamurai* in the fauna last appear at the end of early Tithonian corresponding to top of UAZ 11 of Baumgartner et al. (1995). These taxa are very well-known both from Tethyan and Pacific regions (Dumitrica, 1970; Goriçan, 1994; Baumgartner et al., 1995; Hori, 1999). Disappearance of two taxa (*Sethocapsa accincta* and *Cinguloturris primorika*) had been reported in middle Tithonian (Steiger, 1992; Goriçan, 1994; Kemkin and Taketani, 2004). As these taxa have not been determined and found in many regions, we prefer the early Tithonian age for the upper limit of the fauna.

According to previous study (Baumgartner et al., 1995), although *Cinguloturris cylindra* appear for the first time at early late Tithonian (basal part of UAZ 12), Kemkin and Taketani (2004) reported the presence of it in middle Oxfordian to upper Tithonian strata. Therefore we accepted the total range of *Cinguloturris cylindra* as middle Oxfordian to late Valanginian.

Based on these assumptions, it can be concluded that the age of the sample UKF-14 from the Intra-Pontide mélange prism is late Kimmeridgian to early Tithonian corresponding to UAZ 11 of Baumgartner et al. (1995) (Fig. 10).

DISCUSSION

The initial suggestion of Şengör and Yılmaz (1981) and Yılmaz (1990) is that the IPO formed during the Jurassic between the Eurasian continent to the north and the Sakarya microcontinent to the south and closed in Early Tertiary.

Göncüoğlu et al. (1987, 1997) and Göncüoğlu and Erendil (1990) suggest an older (Late Triassic) opening age. Pelagic limestone blocks with planktic foraminifers of Late Cretaceous (Santonian) age within the mélanges is taken as an evidence that the ocean was in existence by the Late Cretaceous (e.g., Okay and Tüysüz, 1999; Robertson and Ustaömer, 2004). However, it is not clear whether these blocks are really part of the IPS or if they are later reworked from an overlying unit (e.g., Greber, 1997; Beccaletto et al., 2005). Moreover, the presence of an oceanic basin between the Rhodope - Pontide and Sakarya micro-continents is disputed (Elmas and Yigitbas 2001, 2005). Elmas and Yigitbas (2001; 2005) suggest that "the ophiolite blocks must be derived from either the Precambrian metaophiolites in the basement of Istanbul - Zonguldak unit or Palaeotethys" and were transported by the left-lateral strike-slip faults during the Late Cretaceous.

The new data obtained by this study is indicative for basaltic rocks within the IPO formed from a depleted MORB source (spinel lherzolite source) by 5-10% partial melting and fractional crystallization processes. The rocks are distinctly MORB, formed by sea floor spreading. The $(^{143}Nd/^{144}Nd)_i$ data on the other hand suggests that the source was not homogenous. This heterogeneity can be best explained by an earlier subduction. The foremost candidate is the oceanic crust of the Upper Paleozoic - Triassic Tethys (Palaeotethys) that subducted beneath the Sakarya microcontinent (Göncüoğlu et al., 2000).

Limited geochemical data for MORB and OIB-type volcanic rocks were obtained by Robertson and Ustaömer (2004) from the mélanges to the east of Armutlu Peninsula, about 150 km to the west of the study area. The mélange complex in this area includes highly sheared serpentinites, gabbros, meta-basalts and red ribbon cherts (Göncüoğlu et al., 1987). Two samples taken from meta-basic rocks of the Upper Cretaceous Alacam Mélange in the Armutlu Peninsula (Robertson and Ustaömer, 2004; Ustaömer and Robertson, 2005) were evaluated together with our data from the Bolu area on Zr/Y-Zr diagram (Fig. 8). These Alacam Mélange samples roughly plot on the MORB-field. However, the MORB normalized multi-element pattern of the Alacam Mélange clearly differs from the Bolu samples. They are enriched in LREE and display negative Nb anomaly and interpreted as subduction-related basalts by Robertson and Ustaömer (2004). There is no direct evidence for the age of the basalts except that one micritic limestone knocker in the mélange includes *Globotruncana* sp. (Göncüoğlu et al., 1987; 1992; Göncüoğlu and Erendil, 1990). Based on this evidence, the mélange must have been derived from the Neotethys and unrelated to the Precambrian or Paleotethyan ophiolites as advocated by Kaya (1977) or Elmas and Yigitbas (2001; 2005).

The age of the MOR basalts are more precisely dated in this study by radiolarians. Our new findings demonstrate a Late Jurassic (late Kimmeridgian to early Tithonian) age for the basalt formation. Beccaletto et al. (2005) have also reported recently the radiolarian assemblage with *Transhsuum brevicostatum* (Ozvoldova), *Parahsuum* sp. S (sensu Baumgartner et al., 1995), *Tethysetta dhimenaensis dhimenaensis* Baumgartner, *Archaeodictyomitra* (?) *amabilis* Aita, *Stichocapsa robusta* Matsuoka, *Protunuma japonicus* Matsuoka and Yao indicating late Bathonian - early Callovian time interval from the Arkotdağ Mélange. However, the age of this single sample from an unknown locality and geological setting, is slightly older than the radiolarian assemblage described in this study. From "an additional sample of pelagic limestone in Couches Rouges facies from the same locality" these authors reported the pelagic foraminifer fauna with *Dicarinella asymetrica* (Sigal), *D. concavata* (Brotzen), *Globotruncanita elevata* (Brotzen), *Marginotruncana coronata* (Bolli) and *M. pseudolinneiana* Pessagno indicating a Santonian age.

Interestingly, in the Cetmi Mélange in the Biga Peninsula the same authors (Beccaletto et al., 2005) have obtained from the mudstone and radiolarites six different radiolarian assemblages with ages of late Bajocian - early Bathonian, latest Bajocian - early Tithonian, late Oxfordian - Hauterivian, middle Oxfordian - early Tithonian, Tithonian - earliest Berriasian Hauterivian - Aptian. Based on these assemblages, the authors suggest that pelagic sedimentation occurred during late Bajocian to Aptian in an oceanic basin. However, they put forward that the Cetmi Mélange is the western continuation of the Izmir - Ankara Suture and cannot be correlated with the mélanges of the Intra-Pontide suture. The "decisive point" for this statement is, according to Beccaletto et al. (2005), "the younger age of the Izmir - Ankara mélanges". This statement is not in accordance with the data from the Izmir - Ankara Suture in NW Anatolia, as Bragin and Tekin (1996), Göncüoğlu et al. (2000; 2006a; 2006b; 2007), Tekin et al. (2002, 2006), Yalınız and Göncüoğlu (2005) and Tekin and Göncüoğlu (2007) have proven by radiolarian findings and geochemical data that this ocean was open from late Ladinian to early Turonian. By this, the Izmir-Ankara and the Intra-Pontide oceanic branches of the Neotethys coexisted at least from Late Jurassic onwards. Moreover, the Cetmi Mélange in Biga Peninsula may well represent the westernmost outcrops of the IPS, as initially proposed by Göncüoğlu et al. (1997).

CONCLUSIONS

To the east of Bolu within the North Anatolian Fault Zone, discontinuous tectonic slivers of an ophiolitic mélange occur between the crustal assemblages of the Rhodope - Pontide and Sakarya Composite terranes. One of these slivers comprises pillow-lavas, alternating with massive lavas and cut by diabase dykes. The pillow basalts are interlayered with radiolarian cherts and silicified mudstones. Geochemical evaluation of these basalts based on major, trace and REE elements indicates a single and chemically coherent suite displaying tholeiitic affinity. The trace and REE ratios as well as the tectonomagmatic discrimination diagrams are indicative for N-MORB type volcanism. The petrological evaluation suggests that basalts were derived from depleted MORB source (spinel lherzolite source) by 5-10% partial melting and fractional crystallization processes.

The $(^{143}Nd/^{144}Nd)_i$ ratios of the studied samples, ranging from 0.512471 to 0.512786, are lower than the Nd isotopic data of the N-MORB. This is ascribed to the heterogeneity of the source, possibly triggered by the Triassic subduction of the Paleo-Tethys.

Moderately preserved but diverse radiolarians were obtained from silicified mudstones in the upper part of the measured section. This level is dated as late Kimmeridgian to early Tithonian corresponding to UAZ 11 of Baumgartner et al. (1995).

This finding evidences that the MOR-type basalts were generated in the Intra-Pontide Ocean during the Late Jurassic.

A correlation with previous fossil findings along the Intra-Pontide suture belt in NW Anatolia suggests that the Intra-Pontide Ocean existed at least between late Bathonian to Santonian.

The available evidence suggests that the western continuation of the Intra-Pontide suture belt can be followed from Bolu via southern Armutlu to western Biga Peninsula.

More detailed sampling of the radiolarian cherts combined with geochemical evaluation of the volcanic rocks may help to better understand the geological history of this little-known branch of Neotethys in NW Anatolia.
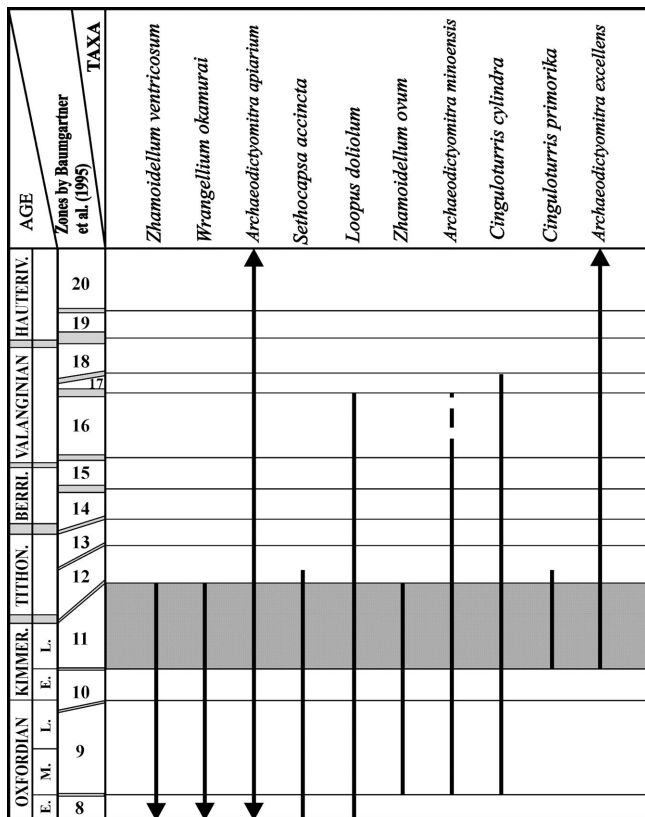

Fig. 10 - Stratigraphic ranges of radiolarian taxa obtained from sample UKF-14 from Kocacay Valley based on studies of Dumitrica (1970), Yao (1984), Steiger (1992), Gorican (1994), Baumgartner et al. (1995), Dumitrica et al. (1997), Hori (1999) and Kemkin and Taketani (2004). Grey area shows the supposed age of assemblage as late Kimmeridgian – early Tithonian.

REFERENCES

Baker J.A., Menzies M.A., Thirlwall M.F. and Macpherson C.G., 1997. Petrogenesis of Quarternary intraplate volcanism, San'a, Yemen: implications for plume-lithosphere interaction and polybaric melt hybridization. J. Petrol., 38: 1359-1390.

Baumgartner P.O., O'Dogherty L., Goriçan S. et al., 1995. Radiolarian catalogue and systematics of Middle Jurassic to Early Cretaceous Tethyan genera and species. In: Baumgartner P.O. et al. (Eds), Middle Jurassic to Lower Cretaceous radiolaria of Tethys: Occurrences, systematics, biochronology. Mém. Géol. Lausanne, 23: 37-685.

Beccaletto L., Bartolini A.C., Martini R., Hochuli P.A. and Kozur H., 2005. Biostratigraphic data from the Cetmi Mélange, northwest Turkey: Palaeogeographic and tectonic implications. Palaeo. Palaeo. Palaeo., 221: 215-244.

Blumenthal M.M., 1949. Bolu civari ile Asagı Kızılırmak mecrasi arasındakı kuzey Anadolu silsilelerinin jeolojisi. M. T. A. Publ., Series B, 13: 1-53.

Bragin N.Yu. and Tekin U.K., 1996. Age of radiolarian-chert blocks from the Senonian ophiolitic mélange (Ankara, Turkey). Island Arc, 5: 114-122.

Chauvel C. and Blichert-Toft J., 2001. A hafnium isotope and trace element perspective on melting of the depleted mantle. Earth Planet. Sci. Lett., 190: 137-151.

Coish R.A. and Sinton C.W., 1992. Geochemistry of mafic lavas in the Adirondack mountains: implications for late Proterozoic continental rifting. Contrib. Mineral. Petrol., 110: 500-514.

Dumitrica P., 1970. Cryptocephalic and Cryptothoracic Nasseleria in some Mesozoic deposits of Romania. Rev. Roum. Géol., Géophys. Géogr. (Série Géol.), 14 (1): 45-124.

Dumitrica P., Immenhauser A. and Dumitrica-Jud R., 1997. Mesozoic radiolarian biostratigraphy from Masirah ophiolite, Sultanate of Oman, Part 1. Middle Triassic, Uppermost Jurassic and Lower Cretaceous spumellarians and multisegmented nassellarians. Bull. Nat. Mus. Nat. Sci., Taiwan, 9: 1-106.

Dupré B. and Allègre C.J., 1980. Pb-Sr-Nd isotopic correlation and the chemistry of the North Atlantic mantle. Nature, 286: 17-22.

Elmas A. and Yigitbas E., 2001. Ophiolite emplacement by strike–slip tectonics between the Pontide Zone and the Sakarya Zone in northwestern Anatolia, Turkey. Int. J. Earth Sci. (Geol. Rundsch.), 90: 257-269.

Elmas A. and Yigitbas E., 2005. Comment on "Tectonic evolution of the Intra-Pontide suture zone in the Armutlu Peninsula, NW Turkey" by Robertson and Ustaömer. Tectonophysics, 405: 213-221.

Elmas A., Yigitbas E. and Yılmaz Y., 1997. The geology of the Bolu - Eskipazar zone: an approach to the development of the Intra-Pontide Suture. Geosound, 30: 1-14.

Floyd P. A., Kelling G., Gokcen S.L. and Gokcen S., 1991. Geochemistry and tectonic environment of basaltic rocks from the Misis ophiolitic mélange, south Turkey. Chem. Geol. 89: 263-280.

Floyd, P.A. and Winchester, J.A., 1975. Magma type and tectonic setting discrimination using immobile elements. Earth Planet. Sci. Lett., 27: 211-218.

Floyd P.A. and Winchester J.A., 1978. Identification and discrimination of altered and metamorphosed volcanic rocks using immobile elements. Chem. Geol., 21: 291-306.

Floyd P.A., Winchester J.A., Seston R., Kryza R. and Crowley Q.G., 2000. Review of geochemical variation in Lower Palaeozoic metabasites from the NE Bohemian Massif; intracratonic rifting and plume ridge interaction. In: W. Franke, V. Haak, O. Oncken and D. Tanner (Eds.), Orogenic processes: Quantifications and modeling in the Variscan Belt. Geol. Soc. London Spec. Publ., 179: 155-174.

Göncüoğlu M.C. and Erendil M., 1990. Pre-Late Cretaceous tectonic units of the Armutlu Peninsula. Proceed. 8th Turk. Petrol. Congr., 8: 161-168.

Göncüoğlu M.C., Dirik K. and Kozlu H., 1997. General characteristics of pre-Alpine and Alpine terranes in Turkey: Explanatory notes to the terrane map of Turkey. Ann. Geol.. Pays Héllén., 37: 515-536.

Göncüoğlu M.C., Erendil M., Tekeli O., Aksay A., Kuscu A. and Ürgün B., 1992. Introduction to the geology of the Armutlu Peninsula. ISGB-92, Guide Book, Ankara, p. 26-36.

Göncüoğlu M.C., Erendil M., Tekeli O., Aksay A., Kuscu A. and Ürgün B., 1987. Geology of the Armutlu Peninsula. Correlations of Variscan and Pre-Variscan events in the Alpine - Himalayan mountain belt. Field meeting. Turkey. Guide book for the field excursion along Western Anatolia, Turkey, Ankara, 5: 12-18.

Göncüoğlu M.C., Turhan N., Senturk K., Ozcan A. and Uysal S., 2000. A geotraverse across NW Turkey: tectonic units of the Central Sakarya region and their tectonic evolution. In: E. Bozkurt et al. (Eds.), Tectonics and magmatism in Turkey and the surrounding area. Geol. Soc. London Spec. Publ., 173: 139-161.

Göncüoğlu M.C., Yalınız M.K. and Tekin U.K., 2006a. Geochemistry, tectono-magmatic discrimination and radiolarian ages of basic extrusives within the Izmir-AnkaraSuture Belt (NW Turkey): Time constraints for the Neotethyan evolution. Ofioliti, 31: 25-38.

Göncüoğlu M.C., Yalınız M.K. and Tekin U.K., 2006b. Geochemical features and radiolarian ages of volcanic rocks from the Izmir-Ankara Suture Belt, western Turkey. Mesozoic ophiolite belts of the northern part of the Balkan Peninsula, Proceed., p. 41-44.

Göncüoğlu M.C., Tekin U.K. and Yalınız M.K., 2007. Tectono-magmatic discrimination and ages of basaltic olistoliths within the Neotethyan Izmir-Ankara Mélange, NW Turkey. Geoitalia 2007, Epitome, 2: 134.

Goriçan S., 1994. Jurassic and Cretaceous radiolarian biostratigraphy and sedimentary evolution of the Budva Zone (Dinarides, Montenegro). Mém. Géol. Lausanne, 18: 1-120.

Greber E., 1997. Stratigraphic evolution and tectonics in an area of high seismicity: Akyazi/Adapazari (Pontides, Northwestern Turkey). In: C. Schindler and M. Pfister (Eds.), Active tectonics of northwestern Anatolia - the Marmara poly-project. VDF Zürich, p. 141-160.

Hart W.K., Wolde G., Walter R.C. and Mertzman S.A., 1989. Basaltic volcanism in Ethiopia: constraints on the continental rifting and mantle interactions. J. Geophys. Res., 94: 7731-7748.

Hoernle K., 1998. Geochemistry of Jurassic oceanic crust beneath Gran Canaria (Canary Islands): implications for crustal recycling and assimilation. J. Petrol., 39: 859-880.

Hofmann A.W., 1989. Geochemistry and models of mantle circulation. Phil. Trans. R. Soc. London, 328: 425-439.

Hofmann A.W., 2003. Sampling mantle heterogeneity trough oceanic basalts: isotopes and trace elements. In: R.W. Carlson, H.D. Holland and K.K. Turekian (Eds.), Treatise on geochemistry, Vol. 2: The Mantle and Core, Elsevier-Pergamon, Oxford, p. 61-101.

Hori N., 1999. Latest Jurassic radiolarians from the northeastern part of the Torinoko Block, Yamizo Mountains, central Japan. Sci. Rep. Inst. Geosci. Univ. Tsukuba, Sec. B., 20: 47-114.

Kamenetsky V.S., Everard J.L., Crawford A.J., Varne R., Eggins S.M. and Lanyon R., 2000. Enriched end-member of primitive MORB melts: petrology and geochemistry of glasses from Macquarie Island (SW Pacific). J. Petrol., 41: 411-430.

Kaya O., 1977. Gemlik Orhangazi alanının Paleozoyik temel yapısına yaklasım. Yerbilimleri, 3: 115-128 (in Turkish with English abstract).

Kaya O. and Kozur H., 1987. A new and different Jurassic to Early Cretaceous sedimentary assemblage in northwestern Turkey (Gemlik, Bursa): implications for the pre-Jurassic to Early Cretaceous tectonic evolution. Yerbilimleri, 14: 253-268.

Kemkin I.V. and Taketani Y., 2004. New radiolarian species from Late Jurassic chert-terrigenous deposits of the Taukha Terrane, southern Sikhote-Alin. Paleont. Res., 8 (4): 325-336.

Köksal S. and Göncüoğlu M.C., 2008. Sr and Nd isotopic characteristics of some S-, I- and A-type granitoids from Central Anatolia. Turk. J. Earth Sci., 17: 111-127.

Leeman W.P. and Hawkesworth C.J., 1986. Open magma systems: trace element and isotopic constraints. J. Geophys. Res., 91: 5901-5912.

Moix P., Beccaletto L., Kozur H.W., Hochard C., Rosselet F. and Stampfli G.M., 2008. A new classification of the Turkish terranes and sutures and its implication for the paleotectonic history of the region. Tectonophysics, 451: 7-39.

Okay A.I. and Tüysüz O., 1999. Tethyan sutures of northern Turkey. In: B. Durand, J L. Olivet, E. Horvath and M. Serrane (Eds.), The Mediterranean basins, extension within the Alpine Orogen. Geol. Soc. London Spec. Publ., 156: 475-515.

Okay A.I., Satir M. and Siebel W., 2006. Pre-Alpide Palaeozoic and Mesozoic orogenic events in the Eastern Mediterranean region. In: D.G. Gee and R.A. Stephenson (Eds.), European lithosphere dynamics. Geol. Soc. London Mem., 32: 389-405.

Okay A.I., Satir M., Maluski H., Siyako M., Monie P., Metzger R. and Akyüz R., 1996. Paleo- and Neo-Tethyan events in northwest Turkey: Geological and geochronological constraints. In: A. Yin and M. Harrison (Eds.), Tectonics of Asia. Cambridge, p. 420-441.

Pearce J.A. and Cann J.R., 1973. Tectonic setting of basic volcanic rocks determined using trace element analyses. Earth Planet. Sci. Lett., 19: 290-300.

Pearce J.A. and Norry M.J., 1979. Petrogenetic implications of Ti, Zr, Y and Nb variations in volcanic rocks. Contrib. Mineral. Petrol., 69: 33-47.

Rehkämper M. and Hofmann A.W., 1997. Recycled ocean crust and sediment in Indian Ocean MORB. Earth Planet. Sci. Lett., 147: 93-106.

Robertson A.H.F., 2004. Development of concepts concerning the genesis and emplacement of Tethyan ophiolites in the Eastern Mediterranean and Oman regions. Earth Sci. Rev., 66: 331-387.

Robertson A.H.F. and Ustaömer T., 2004. Tectonic evolution of the Intra-Pontide suture zone in the Armutlu Peninsula, NW Turkey. Tectonophysics, 381: 175-209.

Rudge J.F., Mc Kenzie D. and Haynes P.H., 2005. A theoretical approach to understanding the isotopic heterogeneity of mid-ocean ridge basalt. Geochim. Cosmochim. Acta, 69: 3873-3887.

Şengör A.M.C. and Yılmaz Y., 1981. Tethyan evolution of Turkey: a plate tectonic approach. Tectonophysics, 75:181-241.

Şengör A.M.C., Yılmaz Y. and Sungurlu O., 1984. Tectonics of the Mediterranean Cimmerides: nature and evolution of the western termination of Palaeo-Tethys. In: J.E. Dixon and A.H.F. Robertson (Eds.), Geological evolution of the Eastern Mediterranean. Geol. Soc. London Spec. Publ., 17: 77-112.

Sevin M., Altun I.E. and Aksay A., 2002. 1/100 000 scaled geological maps Nr. Bolu G27. Publ. of General Directorate of Mineral Research and Exploration, Ankara, p. 29 (in Turkish).

Sobolev A.V., Hofmann A.W., Kuzmin D.V., Yaxley G.M., Arndt N.T., Chung S., Danyushevsky L.V., Elliott T., Frey F.A., Garcia M.O., Gurenko A.A., Kamenetsky V. S., Kerr A.C., Krivolutskaya N.A., Matvienkov V.V., Nikogosian I.K., Rocholl A., Sigurdsson I.A., Sushchevskaya N.M. and Teklay M., 2007. The amount of recycled crust in sources of mantle-derived melts. Science, 316: 412-417.

Stampfli G., 2000. Tethyan Oceans. In: E. Bozkurt, J. Winchester and J.A. Piper (Eds.), Tectonics and magmatism in Turkey and the surrounding area. Geol. Soc. London Spec. Publ., 173: 139-161.

Steiger T., 1992. Systematik, Stratigraphie und Palökologie der Radiolarien des Oberjura-Unterkreide-Grenzbereiches im Osterhorn-Trolikum (Nördliche Kalkalpen, Salzburg und Bayern). Zitteliana, 19: 1-188.

Sun S.S. and McDonough W.F., 1989. Chemical and isotopic systematics of oceanic basalts: implications for mantle composition and process. In: A.D. Saunders and M.J. Norry (Eds.), Magmatism in ocean basins. Geol. Soc. London Spec. Publ., 42: 313-345.

Taylor S.R. and Mc Lennan S.M., 1985. The continental crust: Its composition and evolution. Oxford, Blackwell Scientific.

Tekin U.K. and Göncüoğlu M.C., 2007. Discovery of oldest (late Ladinian to middle Carnian) radiolarian assemblages from the Bornova Flysch Zone in western Turkey: Implications for the evolution of the Neotethyan Izmir-Ankara Ocean. Ofioliti, 32 (2): 131-150.

Tekin U.K., Göncüoğlu M.C. and Turhan N., 2002. First evidence of late Carnian radiolarians from the Izmir-Ankara Suture Complex, central Sakarya, Turkey: implications for the opening age of the Izmir-Ankara branch of Neo-Tethys. Geobios, 35 (1): 127-135.

Tekin U.K., Göncüoğlu M.C., Ozkan-Altiner S. and Yalınız M.K., 2006. Dating of Neotethyan volcanics by planktonic fossil faunas, Bornova Flysch Zone, NW Anatolia. TUBITAK Project No: 103Y027, Final Rep.: 1-226 (in Turkish with English abstract).

Thirlwall M.F., Upton B.G. and Jenkins C., 1994. Interaction between continental lithosphere and the Iceland plume- Sr-Nd-Pb isotope chemistry of Tertiary basalts, NE Greenland. J. Petrol., 35: 839-879.

Tokay M., 1973. Geological observations on them North Anatolian Fault Zone between Gerede and Ilgaz. Proceedings of North Anatolian Fault and Earthquakes Symposium. M.T.A. Publ., p. 12-29.

Ustaömer P.A. and Rogers G., 1999. The Bolu Massif: remnant of a pre-Early Ordovician active margin in the west Pontides, northern Turkey. Geol. Mag., 136 (5): 579-592.

Ustaömer T. and Robertson A.H.F., 2005. Reply to discussion contribution by Elmas A. and Yigitbas E. on ''Tectonic evolution of the Intra-Pontide suture zone in the Armutlu Peninsula, NW Turkey'' by Robertson A.H.F. and Ustaömer T. Tectonophysics, 405: 223-231.

Winchester A.J. and Floyd P.A., 1977. Geochemical discrimination of different magma series and their differentiation products using immobile elements. Chem. Geol., 20: 325-343.

Yalınız M.K. and Göncüoğlu M.C., 2005. Petrology of the basic volcanic rocks in the Bornova Flysch Zone: implications for the evolution of western Izmir-Ankara Ocean). TUBITAK Project Final Rep.: 1-74 (in Turkish with English abstract).

Yao A., 1984. Subdivision of the Mesozoic complex in Kii-Yura area, Southwest Japan and its bearing on the Mesozoic basin development in the Southern Chichibu Terrane. J. Geosci. Osaka City Univ., 27: 41-103.

Yigitbas E., Elmas A. and Yılmaz Y., 1999. Pre-Cenozoic tectonostratigraphic components of the western Pontides and their geological evolution. Geol. J., 34: 55-74

Yılmaz Y., 1990. Allochthonous terranes in the Tethyan Middle East: Anatolia and surrounding regions. Philos. Trans. R. Soc. London Ser. A. Math. Phys. Sci., 331: 611-642.

Yılmaz Y., Gözübol A.M. and Tüysüz O., 1982. Geology of an area in and around the Northern Anatolian transform Fault Zone between Bolu and Akyazı. In: A.M. Isıkara and A. Vogel (Eds.), Multidisciplinary approach to earthquake prediction. Friedr. Vieweg and Sohn, Braunsch., p. 45-65.

Yılmaz Y., Genc S.C., Yigitbas E., Bozcu M. and Yılmaz K., 1995. Geological evolution of the late Mesozoic continental margin of Northwestern Anatolia. Tectonophysics, 241: 155-171.

Yılmaz Y., Tüysüz O., Yigitbas E., Genc S.C. and Şengör A.M.C., 1997. Geology and tectonic evolution of the Pontides. In: A.G. Robinson (Ed.), Regional and petroleum geology of the Black Sea and surrounding region. Mem. Am. Ass. Petrol. Geol., 68: 183-226.

Zindler A. and Hart S., 1986. Chemical thermodynamics. Ann. Rev. Earth Planet. Sci., 14: 493-571.
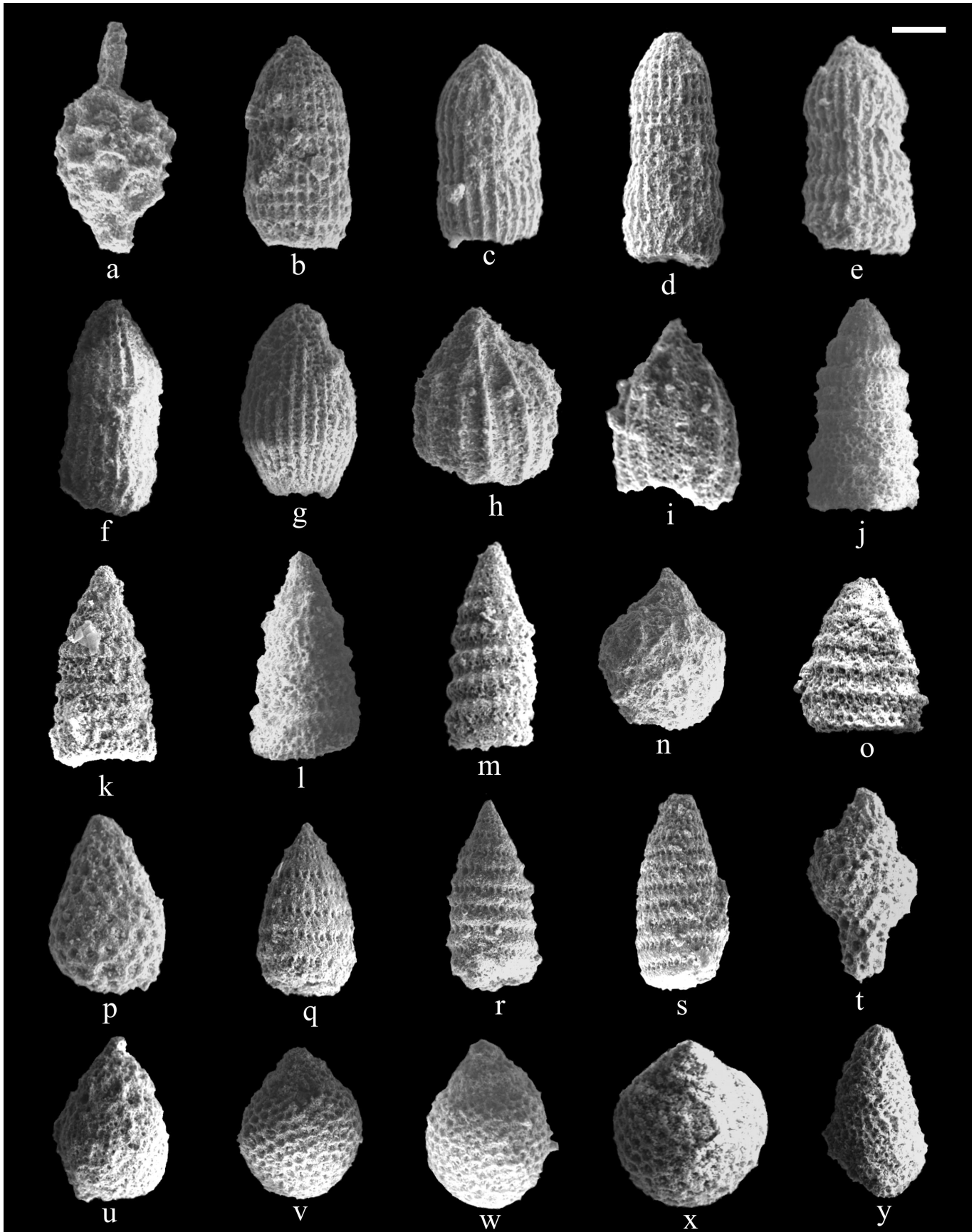
Plate 1 - Scanning electron micrographs of late Kimmeridgian - early Tithonian radiolarians from the sample UKF-14 obtained from Arkotdag Mélange. Scale - number of microns for each figure: a) *Pantanellium* sp., scale bar – 55 µm; b-c) *Archaeodictyomitra apiarium* (Rüst), scale bar, 60 µm; d) *Archaeodictyomitra excellens* (Tan Sin Hok), scale bar, 75 µm; e-f) *Archaeodictyomitra minoensis* (Mizutani), scale bar for both figures, 50 µm; g) *Archaeodictyomitra* sp., scale bar, 50µm; h-i) *Hsuum* ? spp., scale bar, 45 and 40 µm; j-k) *Cinguloturris cylindra* Kemkin and Rudenko, scale bar for both figures, 70 µm; l) *Cinguloturris primorika* Kemkin and Taketani, scale bar, 65 µm; m) *Wrangellium okamurai* (Mizutani), scale bar, 70 µm; n) *Xitus* sp., scale bar, 70 µm; o) *Parvicingula* sp., scale bar, 55 µm; p) *Triversus* sp., scale bar, 35µm; q) *Loopus doliolum* Dumitrica *in* Dumitrica et al., scale bar, 60 µm; r-s) *Loopus* sp., scale bar for both figures, 65 µm; t) *Syringocapsa* sp., scale bar, 75 µm; u) *Sethocapsa accincta* Steiger, scale bar, 70 µm; v-w) *Zhamoidellum ovum* Dumitrica, scale bar for both figures, 45 µm; x) *Zhamoidellum ventricosum* Dumitrica, scale bar, 40 µm; y) *Pseudoeucyrtis* ? sp., scale bar, 60 µm.